

Optical readout of secondary scintillation from liquid argon generated by a thick gas electron multiplier

P.K.Lightfoot ^{a*}, G.J. Barker ^b, K. Mavrokoridis ^a, Y.A. Ramachers ^b, N.J.C. Spooner ^a

^a Department of Physics and Astronomy, University of Sheffield, Hicks Building, Hounsfield Road, Sheffield, S3 7RH, UK

^b Department of Physics, University of Warwick, Coventry, CV4 7AL, UK

Abstract

For the first time secondary scintillation, generated within the holes of a thick gas electron multiplier (TGEM) immersed in liquid argon, has been observed and measured using a silicon photomultiplier device (SiPM).

250 electron-ion pairs, generated in liquid argon via the interaction of a 5.9KeV Fe-55 gamma source, were drifted under the influence of a 2.5KV/cm field towards a 1.5mm thickness TGEM, the local field sufficiently high to generate secondary scintillation light within the liquid as the charge traversed the central region of the TGEM hole. The resulting VUV light was incident on an immersed SiPM device coated in the waveshifter tetraphenyl butadiene (TPB), the emission spectrum peaked at 460nm in the high quantum efficiency region of the device.

For a SiPM over-voltage of 1V, a TGEM voltage of 9.91KV, and a drift field of 2.5KV/cm, a total of 62 ± 20 photoelectrons were produced at the SiPM device per Fe-55 event, corresponding to an estimated gain of 150 ± 66 photoelectrons per drifted electron.

Key words: Electroluminescence, secondary scintillation, proportional light, argon, gas electron multiplier, silicon photomultiplier, neutrino, dark matter.

Corresponding author: Dr. Phil Lightfoot, Department of Physics and Astronomy,

University of Sheffield, Hicks Building, Hounsfield Road, Sheffield S3 7RH, UK,

Tel: +44(0)1142224533, Fax: +44(0)1142223555, E-mail:p.k.lightfoot@sheffield.ac.uk

1. Introduction

The liquid argon time projection chamber (TPC) is a leading technology candidate for the type of large scale underground detector widely acknowledged to be the next-generation project in the areas of neutrino oscillation physics, astro-particle physics and proton decay. The current challenge is to establish methods of tracking and homogeneous calorimetry combining the excellent performance of a liquid argon TPC with a practical implementation that is cost effective and readily scalable up to the benchmark of 100kton.

Charge losses over long drift distances in liquid argon mean that amplification of charge is required. Gas electron multipliers (GEMs) [1], TGEMs [2], Micromegas [3], and Bulk Micromegas [4], have evolved over the last 20 years and are now routinely used within large volume targets. Significant charge amplification within the liquid has however proven difficult to achieve in a practical design [5] leading to the consideration of two-phase liquid argon volumes where the charge amplification using TGEM's occurs in the gas phase above the liquid volume. These designs bring their own problems however and there is a risk the performance could be compromised on the largest scales by the requirements of precise liquid levelling, extreme cooling stability and space-charge effects at the liquid-gas interface.

There is motivation therefore to investigate alternative ways in which a single phase liquid argon volume could be used for 3D tracking and in particular the possibility of using scintillation light readout rather than charge. The successful operation of single phase liquid argon TPC's based on light readout via, for example the imaging of TGEM planes with SiPM arrays, would significantly reduce the complexity of design and allow modular construction of large arrays with readout in any plane.

This report describes the first measurement of secondary scintillation light produced within the holes of a TGEM and viewed by a SiPM device all within a single phase liquid argon target, and builds on an earlier study in which SiPM performance was assessed [6] at cryogenic temperatures.

2. Experimental Details

The liquid argon cryostat used in all tests was contained within a pressurised liquid nitrogen volume. The internal assembly, shown in figure 1, consisted of a 1mm^2 SiPM device positioned directly above the centre of a 65mm diameter TGEM, located above a 20mm drift region defined by a woven steel cathode at the base of the assembly.

The TGEM was manufactured from a double faced copper clad FR-4 epoxy resin glass reinforced composite plate of thickness 1.5mm, hole diameter 1mm, pitch 1.5mm, only the central region of the TGEM being perforated. Two 5mm diameter polystyrene cylinders were fitted between the SiPM and the TGEM to isolate the SiPM device from background scintillation light from the argon target as shown in figure 1.

Although the principle aim was the measurement of secondary scintillation from liquid argon using the SiPM device, satisfactory performance of the TGEM was first confirmed by reading out the charge produced in the gas phase of a double phase argon system at cryogenic temperature. In all cases the bottom face of the TGEM was grounded, a drift field between 1 and 4KV/cm created by applying negative potential to the steel cathode. The amplification field within the TGEM was controlled at the top TGEM electrode and the charge signal, read from the top TGEM electrode, passed through an Amptek A250 charge sensitive preamplifier to an Acqiris CC108 PCI acquisition system triggered through a discriminator unit.

The optical signal was readout using a SensL series 1000 SiPM connected to an external preamplifier. Device characteristics are listed in table 1. The output signal from the SiPM

preamplifier was split, one signal passing directly to an input channel on the Acqiris unit. The other signal was connected through an Ortec 572 shaping amplifier with a 10 μ s integration time, to a N417 discriminator and then to the trigger input of the Acqiris unit.

Table 1. Characteristics of SensL series 1000 SiPM device and associated pre-amp.

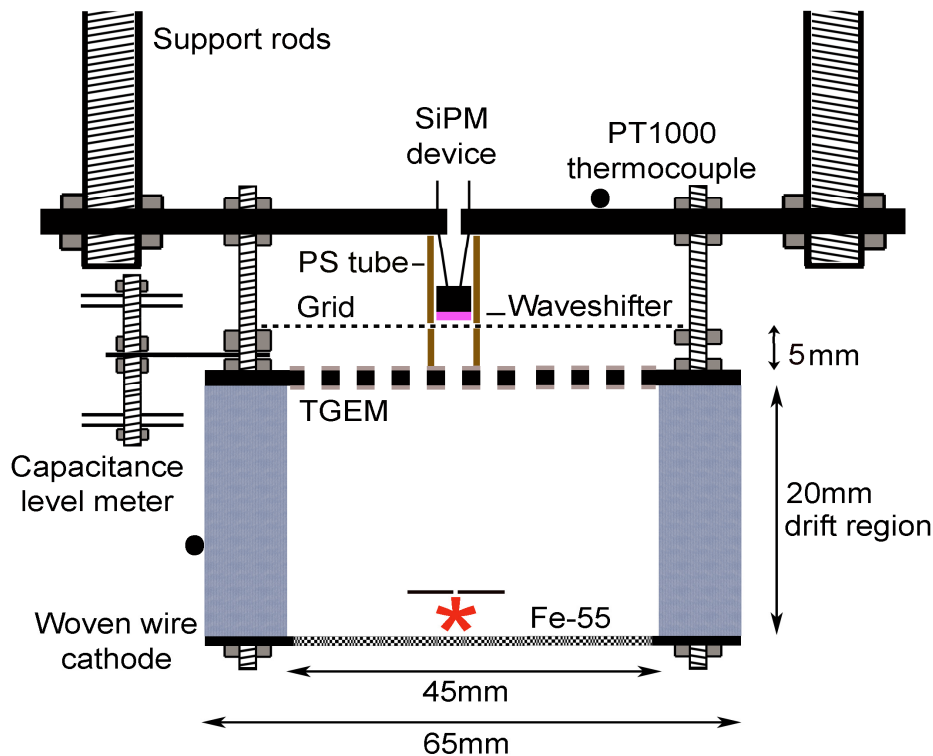
Pixel size	Number of cells	Geometric efficiency %	Maximum gain	Pixel recovery time (ns)	Spectral range (nm)	V _{breakdown} at 25°C
20 μ m	848	43	8 \times 10 ⁶	40ns	400 - 700	28.2V

Prior to all tests the inner chamber was evacuated to 1 \times 10⁻⁸ mbar and baked to 60°C. For all low temperature measurements as liquid nitrogen was slowly added to the cryogenic jacket, the pressure of argon gas within the target was maintained at 1 bar until liquefaction eventually occurred. At this point the cryogenic jacket was filled with liquid nitrogen and pressurized to between 3 and 3.5 bar thereby increasing the boiling point of liquid nitrogen to the point at which liquid argon could condense within the target at 1 bar.

Argon emits VUV scintillation light at 128nm. Light collection was increased by coating the SiPM device with a waveshifter to shift direct 128nm VUV light to 460nm visible light [7] and into the sensitive high quantum efficiency region of the device [6].

Fe-55 (5.9KeV gamma emitter) was positioned at the centre of the steel woven cathode within the drift region, the source collimated using a thin steel sheet to ensure gamma interactions were limited to the vertical axis through the SiPM device. The average number of primary electrons-ion pairs generated from a 5.9 KeV Fe-55 source assuming a W-value of 23.6eV [8] was 250. The ratio of the charge collected at the top TGEM electrode or the number of secondary photons detected by the SiPM to the charge generated within the drift region was then used to determine the charge gain and optical gain respectively of the TGEM when operated in charge amplification mode or scintillation mode.

Figure 1. Internal assembly used to detect secondary scintillation in liquid argon.



3. Results

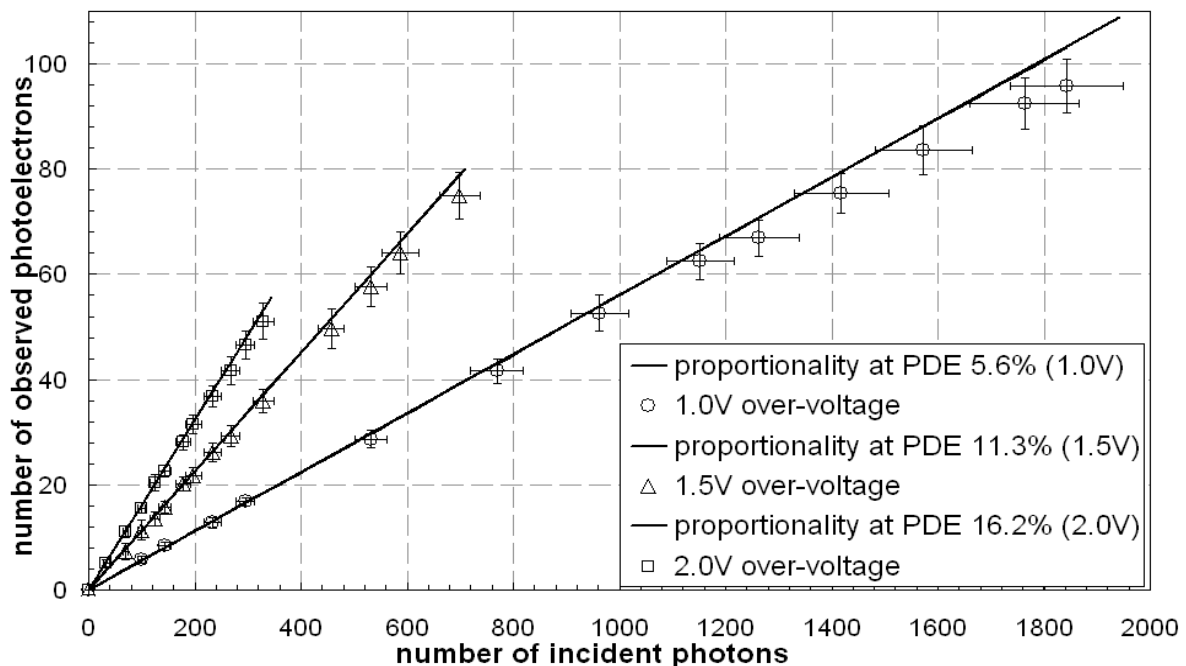
In order to fully characterise the assembly, it was essential to measure the performance of the SiPM device, to ensure that the TGEM was operating correctly and that the argon was of sufficiently high purity to allow charge drift. Following this, the field within the TGEM was varied and secondary scintillation measured as a function of the TGEM field.

3.1 Limit of SiPM device linearity due to saturation effects at high LED photon flux rates

Due to the digital nature of operation, at any time a proportion of the total number of pixels of the SiPM device will be in a state of recovery. This characteristic places a limit on the extent of linearity of the device especially for high intensity pulses of similar time scale to the recovery time. For electron recoils within liquid argon, approximately 23% of all photons are produced within the first 6ns following an interaction, the remaining 77% forming an exponential distribution with a 1590ns time constant [9]. An evaluation of the linearity of the output signal from the SiPM with increasing light intensity was performed at -196°C . Full experimental details are contained in reference [6]. A pulsing circuit [10] was connected to an externally mounted light emitting diode (LED) producing 5ns rise-time 15ns decay-time light pulses of variable intensity, which were passed through a fibre optic cable to the SiPM device held on a support structure within the target. For a fixed over-voltage, the intensity of the 460nm LED pulse was gradually increased and the output signal recorded.

Measurements show linearity of the output signal is maintained at low incident photon fluxes irrespective of the over-voltage. Data shown in figure 2 indicates a 5% deviation from linearity to occur for a 1V over-voltage for incident fluxes containing in excess of 1500 photons. In all future measurements using argon each scintillation pulse was assessed to ensure that the photon flux within any 40ns window did not exceed the stated 5% deviation limit for the selected over-voltage value.

Figure 2. Linearity of a SiPM device at high LED photon flux rate.



3.2 Cryogenic operation of the TGEM in charge amplification mode in the vapour phase of a double phase argon system

Liquid argon was condensed within the chamber and the TGEM operated in charge gain mode in order to confirm that both the magnitude of the drift field and the degree of purification were sufficient to enable charge transfer through the liquid. By careful addition of argon the liquid level was set so as to produce corresponding fields within the vapour phase below the TGEM of 4.0KV/cm, and within the liquid of 2.5KV/cm.

Measurements, shown in figure 3, were made of the charge gain as a function of the amplification field within the TGEM in 1 bar cold saturated argon gas above the liquid phase. For amplification fields in excess of 18KV/cm, a photopeak was identified due to the internal 5.9KeV Fe-55 source, shown in figure 4. For a constant amplification field, these events were stopped by reduction of the drift field as shown in figure 5, thereby demonstrating that they originated from within the liquid.

Figure 3. Charge gain versus potential across TGEM in 1 bar saturated argon gas above the liquid phase of a double phase system for a 2.5KV/cm constant drift field within the liquid. Room temperature charge gain in 3 bar argon is shown for comparison.

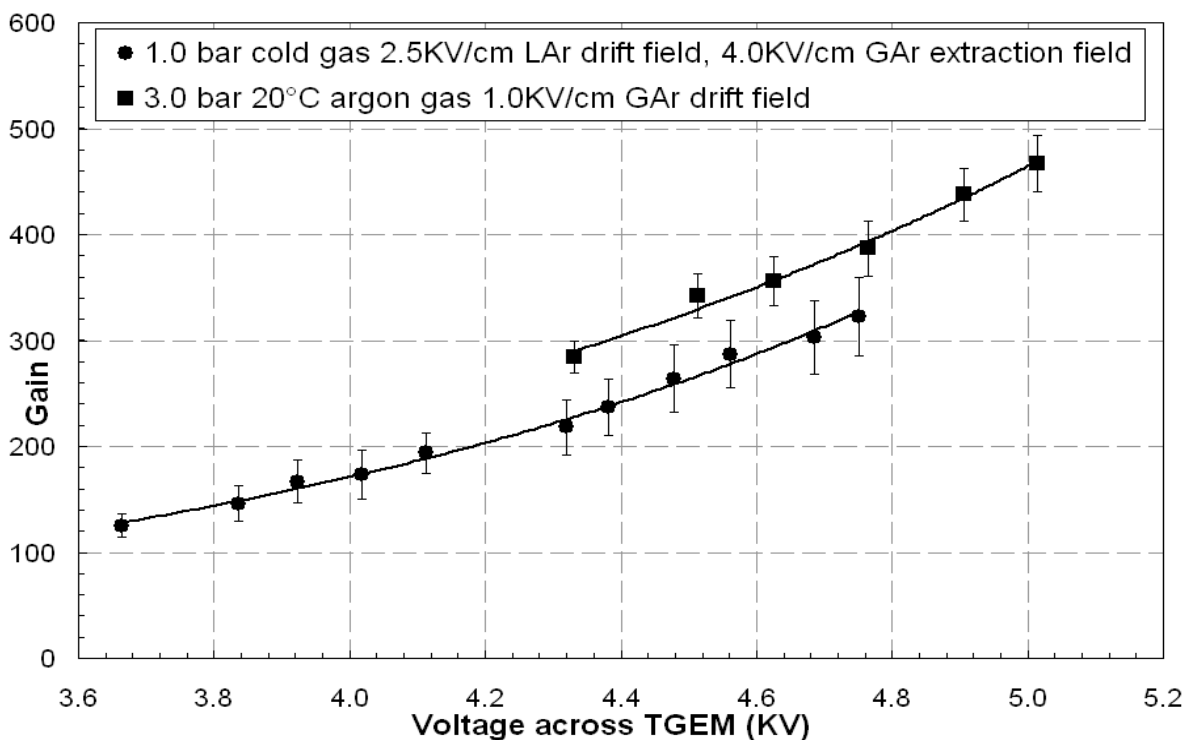


Figure 4. Charge spectrum from Fe-55 in the cold 1 bar gaseous argon phase of a double phase system. ($V_{\text{TGEM}} = 4.685\text{KV}$, Drift field in liquid = 2.5KV/cm and in gas = 4.0KV/cm , gain = 303, 171388 total events.)

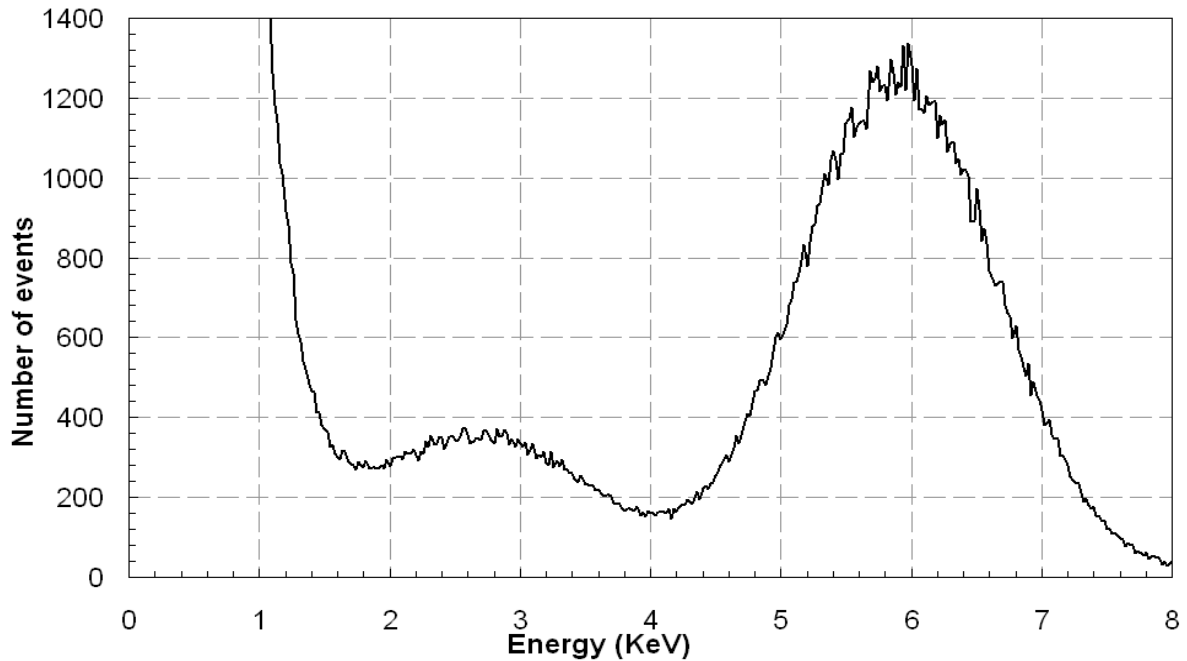
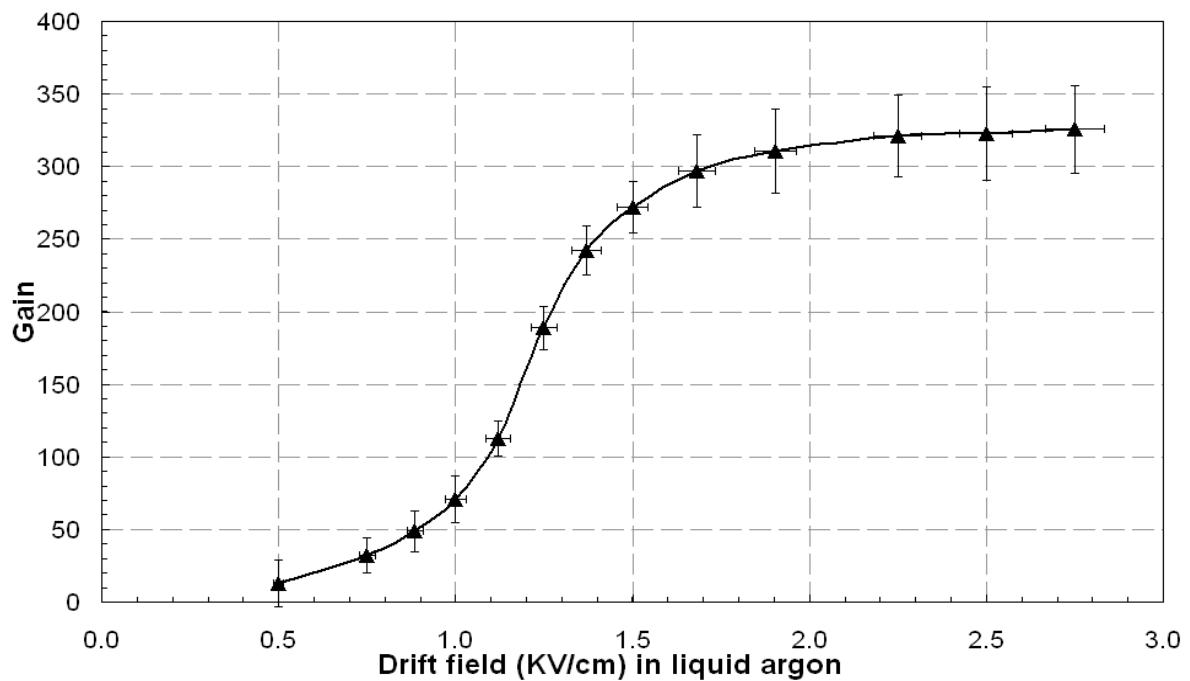


Figure 5. Charge gain versus drift field within liquid argon for a fixed TGEM potential of 4.75KV .



3.3 Cryogenic measurement of secondary scintillation generated within a TGEM in the vapour phase of a double phase argon system using a SiPM device

The SiPM device, now with a breakdown voltage of 24.2V at -189°C [6] was operated at a bias voltage of 25.2V corresponding to an over-voltage of 1V, in 1 bar saturated argon vapour. For a constant drift field of 2.5KV/cm within the liquid phase, the electric field between the TGEM electrodes was steadily increased and the photoelectron pulse distribution produced by the SiPM within a 10 μ s data acquisition time window recorded.

As the field within the TGEM holes increased, secondary scintillation was observed between 2.1KV and 3.4KV. Figure 6 shows a secondary scintillation spectrum for Fe-55 for 2.16KV across the TGEM, the presence of both the argon escape peak (electron binding energy of 3.2KeV) and approximately 12 photoelectron peaks above the discriminator level providing calibration for the 5.9KeV Fe-55 peak. Figure 7 shows light collection as a function of TGEM voltage. Although a linear fit could be applied to the distribution, figure 3 suggests an exponential relationship to be more appropriate. Although the origin of the scintillation pulses can be ascertained from the presence of both the escape peak and the Fe-55 full absorption peak, further evidence can be gleaned from the scintillation response as the drift field is reduced as shown in figure 8.

Figure 6. Secondary scintillation spectrum from Fe-55 in the cold 1 bar gaseous argon phase of a double phase system. (SiPM over-voltage=1V, $V_{TGEM} = 2.16KV$, Drift field in liquid = 2.5KV/cm and in gas = 4.0KV/cm, 5.9KeV peak corresponding to 86 photoelectrons.)

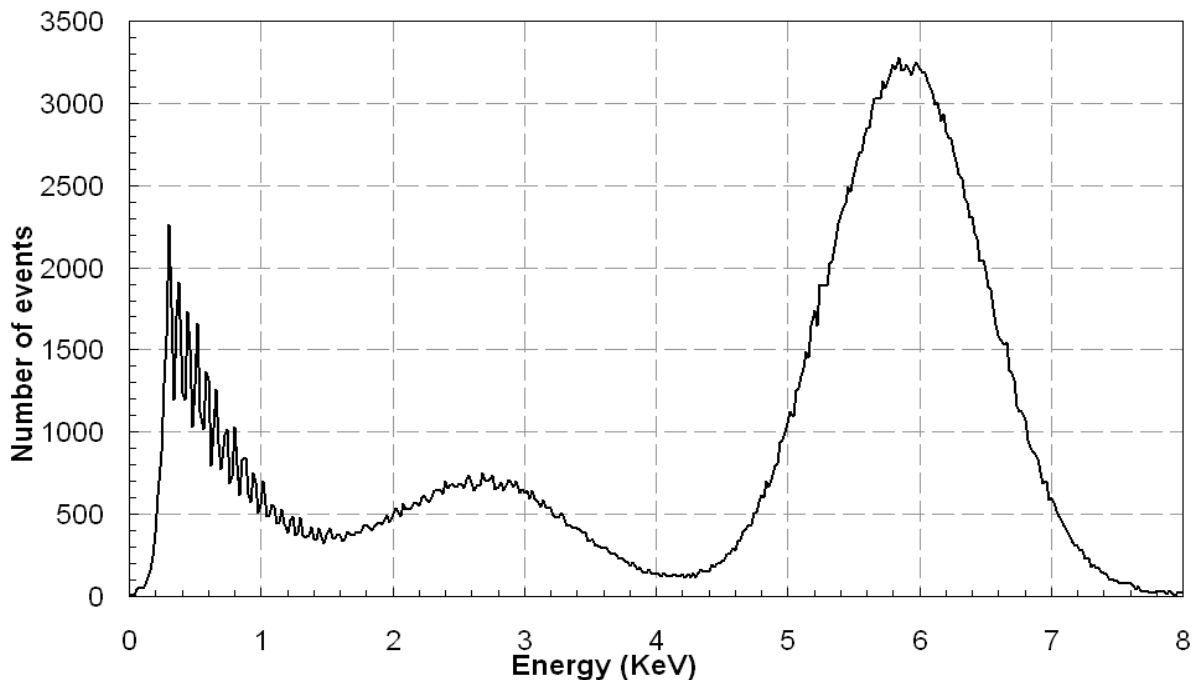


Figure 7. Secondary scintillation in 1 bar -189°C gaseous argon as a function of the voltage across a TGEM due to the passage of charge generated via the interaction of an Fe-55 source in the liquid phase within a 2.5KV/cm drift field.

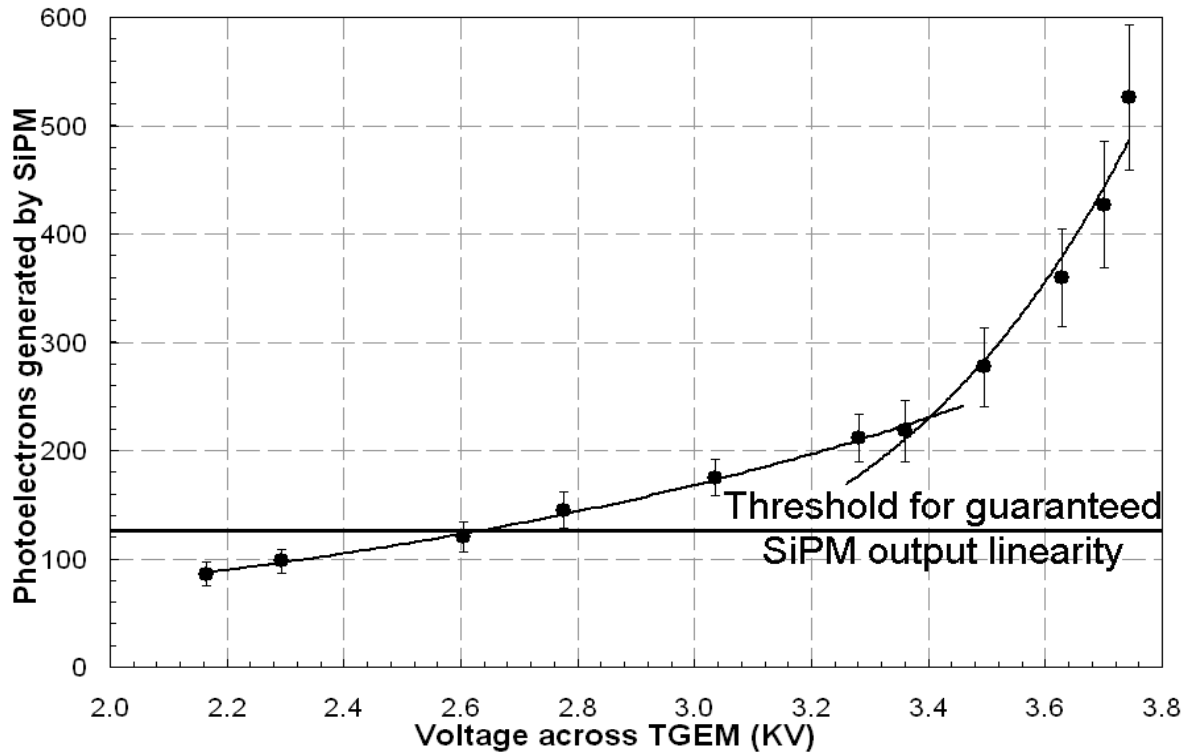
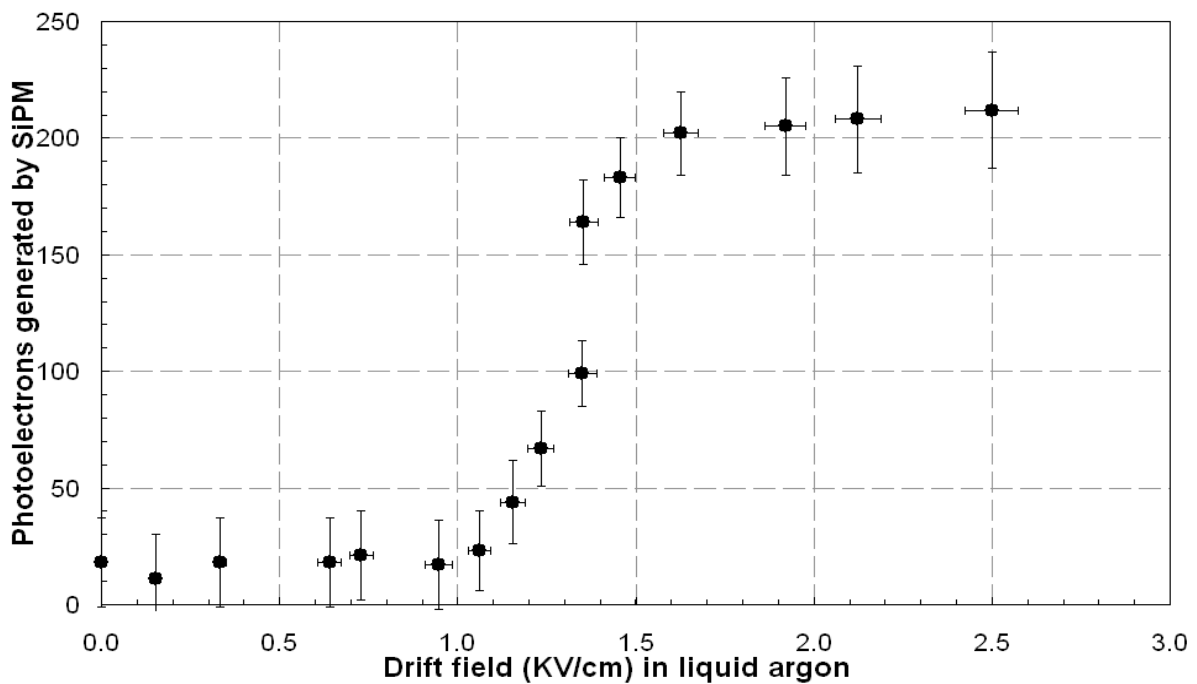


Figure 8. Secondary scintillation versus drift field within liquid argon for a fixed TGEM potential of 3.36KV operating in the cold gas phase of a double phase target.



3.4 Secondary scintillation generated within a TGEM measured using a SiPM device with both immersed in a single phase liquid argon system

Sections 3.2 and 3.3 successfully demonstrated both cryogenic operation of the SiPM device and successful charge transfer through purified liquid argon. Whilst charge amplification in cold argon vapour has already been successfully achieved [11], exhaustive testing failed to generate any measurable charge gain from a TGEM submerged in liquid argon. Following directly from double phase testing, liquefaction was continued until both the SiPM and TGEM were submerged. The drift field was set to 2.5KV/cm and the voltage across the TGEM was slowly increased. At voltages across the TGEM in excess of 8KV the rate and magnitude of the photoelectron pulses became more pronounced. By careful adjustment of both the discriminator threshold level, and the use of a low pass hardware filter, a peak believed to be due to the Fe-55 source was observed at 9.85KV. As the voltage was increased the resolution decreased until at 10.15KV the peak became almost impossible to separate from the background contribution.

The resolution of the Fe-55 signal is degraded in liquid compared to previous measurements in gas. This is believed to be as a consequence of the long 10 μ s integration time required to fully acquire the slow component time constant of 1590ns [9]. Because of the extended decay time compared with for example xenon, each triggered event contains, in addition to an Fe-55 pulse, contributions from primary scintillation due to radioactive background interaction, DCR effects, and crucially photons created due to sparking within the TGEM operating close to the breakdown threshold. With increasing TGEM field, the contribution from these sources increased, reducing the resolution of the Fe-55 pulse above 9.91KV and effectively masking it above 10.15KV. Figure 9 shows a characteristic pulse attributed to Fe-55 at 9.91KV between the TGEM electrodes, whilst figures 10 shows spectra taken for TGEM voltages of 9.91KV. The number of photoelectrons generated at the SiPM as a function of the voltage across the TGEM is shown in figure 11.

Figure 9. A secondary scintillation light pulse produced by an Fe-55 source in a liquid argon system. (SiPM over-voltage=1V, $V_{TGEM} = 9.91KV$, Drift field in liquid = 2.5KV/cm.)

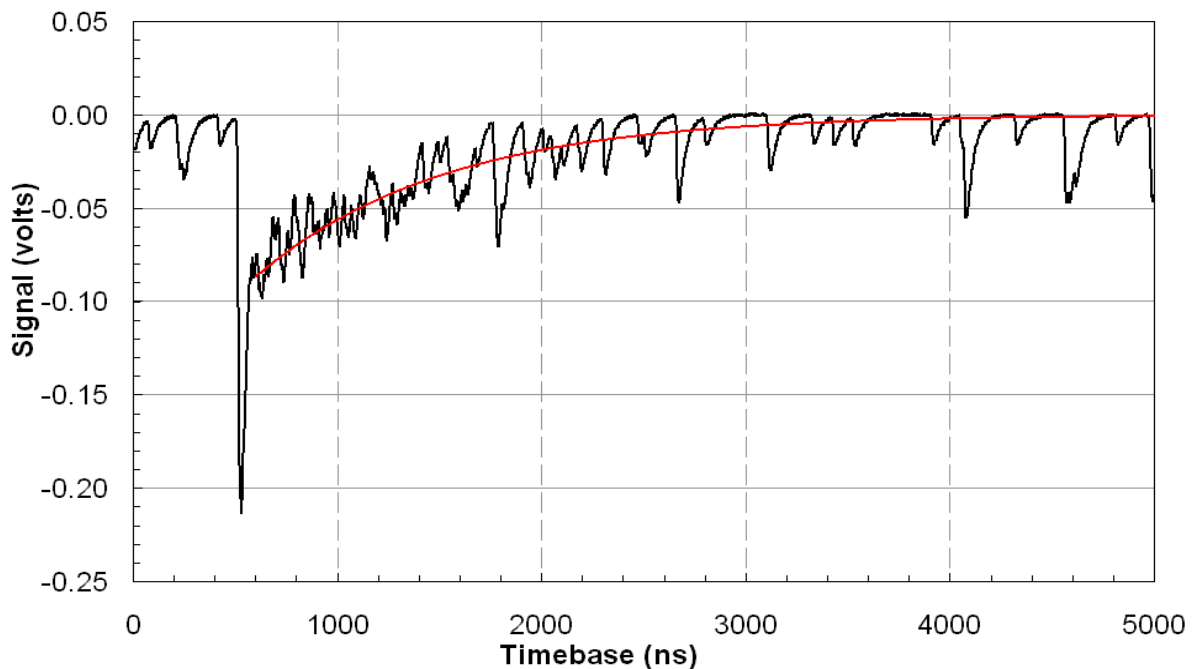


Figure 10. Secondary scintillation spectrum from Fe-55 in a liquid argon system. (SiPM over-voltage=1V, $V_{TGEM} = 9.91KV$, Drift field in liquid = 2.5KV/cm, 5.9KeV peak corresponding to 62 photoelectrons, 1037508 total events.)

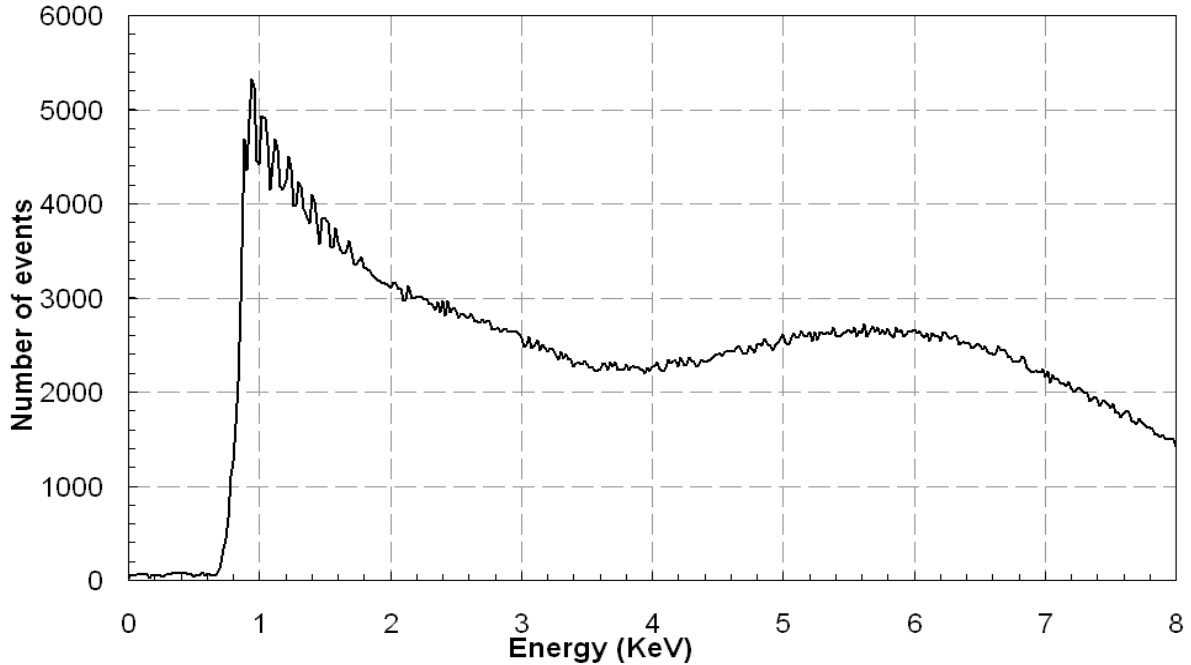
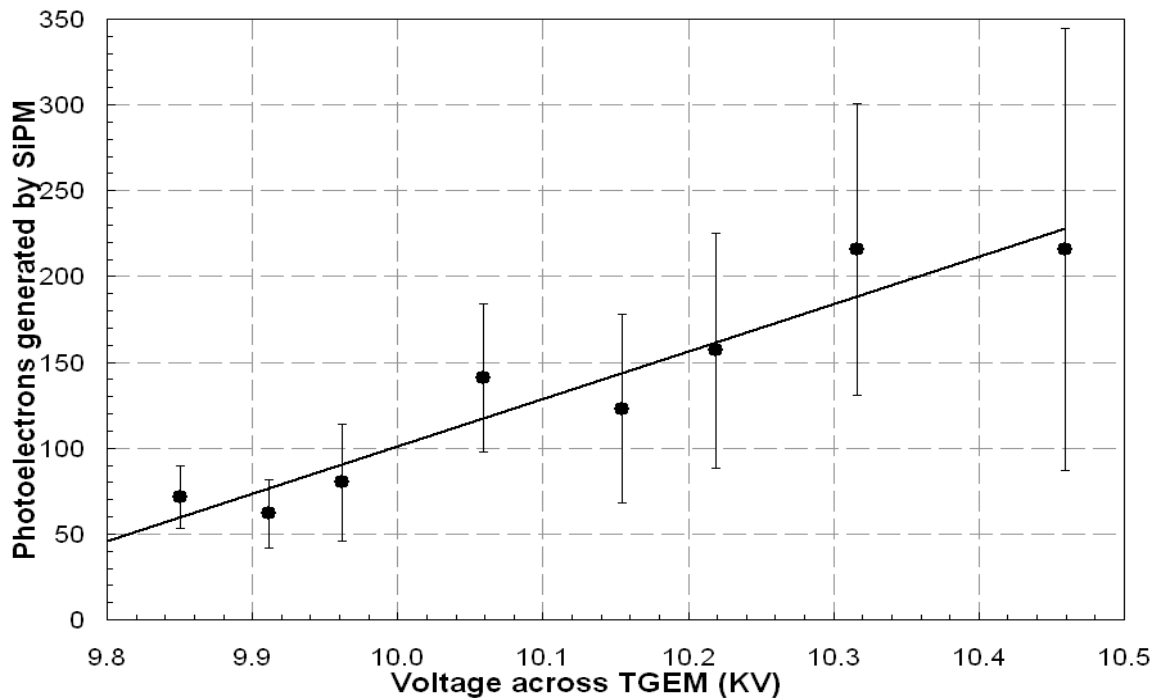


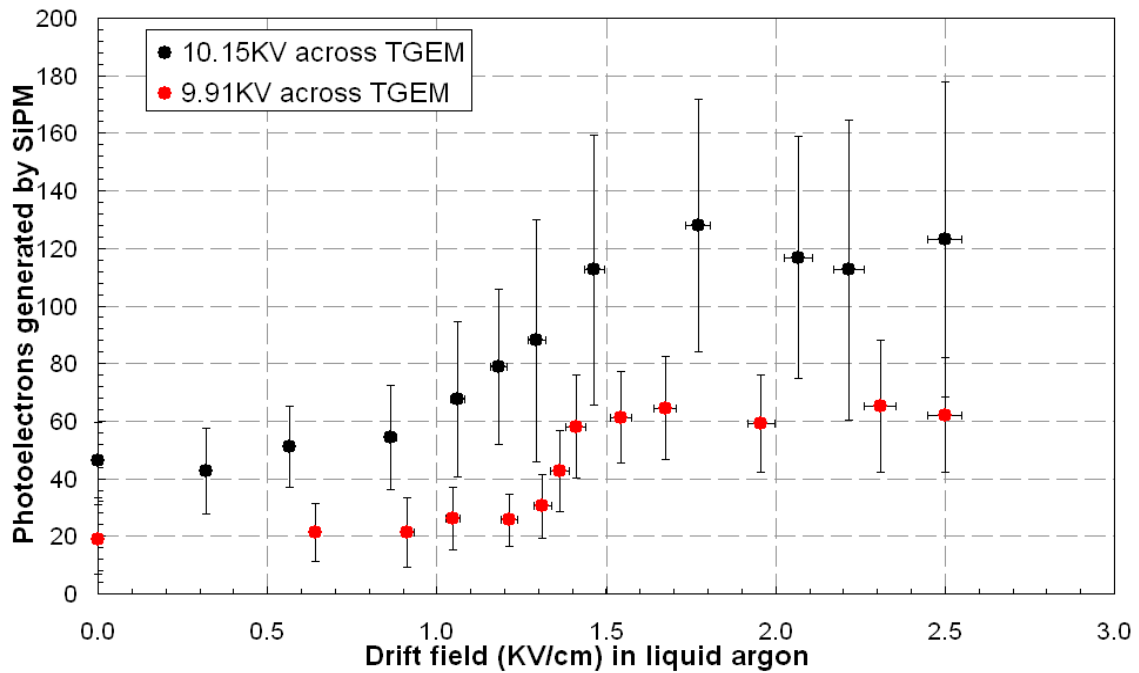
Figure 11. Secondary scintillation generated in liquid argon within a TGEM viewed by a submerged SiPM as a function of voltage across a TGEM at a constant 2.5KV/cm drift field.



The drift field was then reduced from 2.5KV/cm, and the number of photoelectrons collected at the SiPM corresponding to the Fe-55 peak recorded for two applied voltages across the TGEM. Although a reduction in photoelectron collection is observed for both cases, the effect

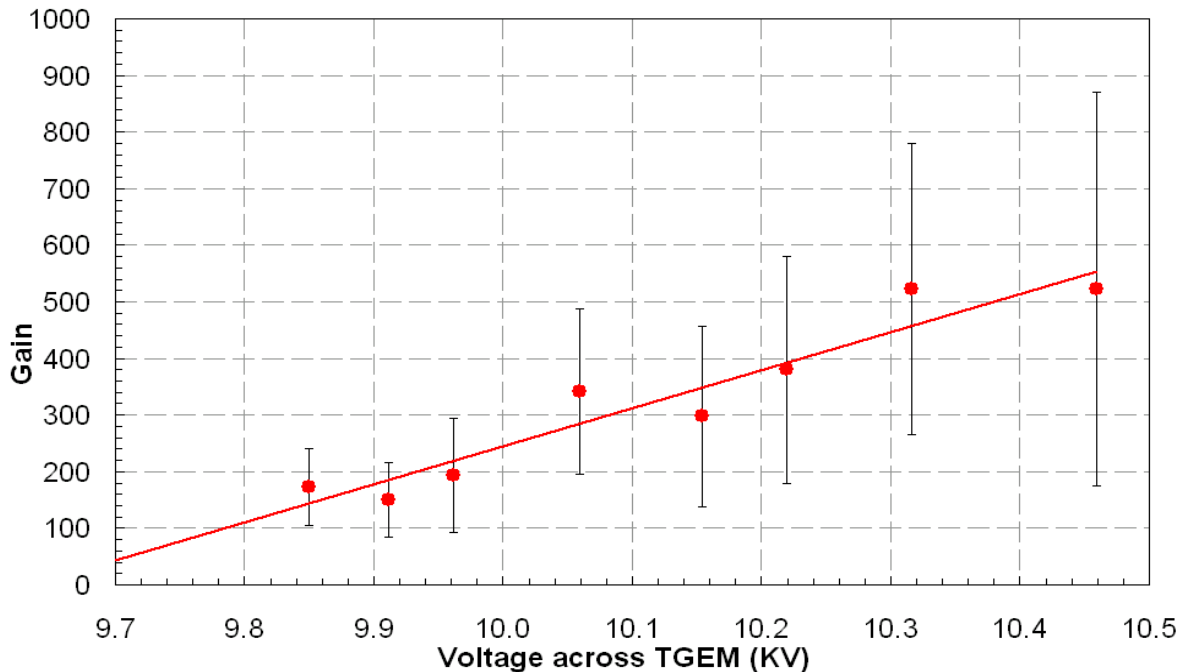
was more pronounced for 9.91KV due to a combination of reduced background noise and greater energy resolution of the Fe-55 peak position. Results are shown in figure 12.

Figure 12. Secondary scintillation corresponding to the Fe-55 peak versus drift field within liquid argon for fixed TGEM potentials of both 9.91KV (red) and 10.15KV (black).



Finally an estimate was made of the photon yield produced at the TGEM shown in figure 13.

Figure 13. Estimated secondary scintillation gain in liquid argon as a function of voltage across the TGEM.



4. Discussion

Studies of charge amplification [5][12] in pure liquid argon have failed to yield any reliable gain. Irrespective of the choice of charge readout device, the maximum charge gain drops with increasing gas pressure and therefore density [13] due to the decrease of the electron impact ionisation yield in the reduced electric field (E/P) within the avalanche region, and the limit due to breakdown imposed on the potential difference between the electrodes.

Although the breakdown limit of a TGEM operating in charge gain mode in pure noble gas is ultimately determined by the effect of UV photon emission, in a heavily optimised system gain is limited by charge build up within the amplification region. The high electric fields required for charge amplification can also lead to charging of the dielectric and ultimately to dielectric breakdown. Additionally, high levels of UV photon emission (secondary scintillation) always associated with charge gain, reduce the device stability, and bubble formation on the sharp edges of the TGEM electrodes can lead to the creation of conducting paths culminating in gaseous discharge.

Secondary scintillation was only observed in gas at TGEM fields for which charge amplification was already established, with the effect that ionisation electrons created in the charge multiplication process then interacting with the medium, yield additional secondary scintillation and therefore an exponential scaling with the applied field. No evidence of charge multiplication was detected during this work for any electric field within liquid argon and it is assumed that the field required to initiate secondary scintillation via excitation is below the ionisation threshold of the medium, the energy dissipated via the emission of UV photons, which do not participate further in the process. Secondary scintillation therefore scales linearly with electric field in the liquid, and may therefore eventually be considered more predictable and less prone to breakdown. Results contained within this report have demonstrated that using secondary scintillation as the readout signal, it is possible to achieve high gains and potentially satisfactory energy resolution from a single TGEM in liquid argon. By operating the TGEM at a lower field in the secondary scintillation proportional mode, detector instability is reduced, and dielectric and UV photon mediated breakdown are avoided. Readout of secondary scintillation also increases signal to noise ratio and reduces the requirements of the front end electronics on the TGEM.

5. Conclusions

For the first time secondary scintillation, generated within the holes of a thick gas electron multiplier (TGEM) immersed in liquid argon, has been observed and measured using a silicon photomultiplier device (SiPM). Secondary scintillation has also been observed in 1 bar cold saturated vapour in a double phase chamber. In both cases the origin of the photon production was ascertained by reduction of the drift field. In order to explain the exponential nature of secondary scintillation generation, measurements of charge gain were taken in gaseous argon, comparison of the voltage range across the TGEM for each process revealing the resulting scintillation gain to be a combination of both.

The combination of the waveshifter tetraphenyl butadiene (TPB) within a gel applied to the surface of the SiPM device was found to efficiently absorb 128nm VUV light produced within the TGEM holes, and to then emit 460nm in the high quantum efficiency region of the device. Overall, for a SiPM over-voltage of 1V, a TGEM voltage of 9.91KV, and a drift field of 2.5KV/cm, a total of 62 ± 20 photoelectrons were produced at the SiPM device per Fe-55 event, corresponding to an estimated gain of 150 ± 66 photoelectrons per drifted electron.

This new liquid argon detection technology is considered to hold great potential on the route to cost-effective, large volume, simultaneous tracking and calorimetry targets with excellent performance relevant to important applications in fundamental particle physics.

References

- [1] F. Sauli, *GEM: A new concept for electron amplification in gas detectors*, Nucl. Instr. and Meth. **A386**, (1997), 531.
- [2] A. Bondar, A. Buzulutskov, A. Grebenuk, D. Pavlyuchenko, R. Snopkov, Y. Tikhonov, V.A. Kudryavtsev, P.K. Lightfoot, N.J.C. Spooner, *A two-phase argon avalanche detector operated in a single electron counting mode*, Nucl. Instr. and Meth. **A574**, (2007), 493.
- [3] P.K. Lightfoot, et al., *Development of a double-phase xenon cell using micromegas charge readout for applications in dark matter physics*, Nucl. Instr. and Meth. **A554**, (2005), 266.
- [4] P.K. Lightfoot, et al., *First operation of bulk micromegas in low pressure negative ion drift gas mixtures for dark matter searches*, Astropart. Phys. **27**, (2007), 490.
- [5] J.G. Kim, et al., *Electron avalanches in liquid argon mixtures*, Nucl. Instr. and Meth. **A534**, (2004), 376.
- [6] P.K. Lightfoot, et al., *Characterisation of a silicon photomultiplier device for applications in liquid argon based neutrino physics and dark matter searches*, **JINST 3**, (2008), P10001.
- [7] K. Mavrokoridis, et al., *Development of wavelength shifter coated reflectors for the ArDM argon dark matter detector*, awaiting submission to JINST.
- [8] M. Miyajima, et al., *Average energy expended per ion pair in liquid argon*, Phys. Rev. **A9**, (1974), 1438.
- [9] A. Hitachi, et al., *Effect of ionization density on the time dependence of luminescence from liquid argon and xenon*, Phys. Rev **B 27**, (1983), 5279.
- [10] J.S. Kapustinsky, R.M. DeVries, N.J. DiGiacomo, W.E. Sondheim, J.W. Sunier, H. Coombes, *A fast timing light pulser for scintillation detectors*, Nucl. Instr. and Meth. **A241**, (1985), 612-613.
- [11] A. Bondar, et al., *Two phase argon and xenon avalanche detectors based on gas electron multipliers*, Nucl. Instr. and Meth. **A556**, (2006), 273.
- [12] S.E. Derenzo, T.S. Mast, R.A. Muller, and H. Zaklad, *Electron avalanche in liquid xenon*, Phys. Rev. A, vol. **9**, (1974), 2582.
- [13] F.D. Amaro, et al., *Operation of a single-GEM in noble gases at high pressure*, Nucl. Instr. and Meth. **A579**, (2007), 62.